Desalination and Water Treatment
www.deswater.com

doi: 10.1080/19443994.2016.1148220

57 (2016) 23074–23084
October

Taylor & Francis
Taylor & Francis Group

MED seawater desalination using a low-grade solar heat source

Philippe Bandelier[a,*], Frédéric Pelascini[b], Jean-Jacques d'Hurlaborde[c], Amélie Maisse[a], Benjamin Boillot[a], Jordan Laugier[a]

[a]*CEA-Liten, 17 rue des Martyrs, 38054 Grenoble, France, Tel. +33 438 784 221; email: philippe.bandelier@cea.fr (P. Bandelier)*
[b]*CRITT Matériaux Alsace, 19 rue de saint Junien, 67305 Schiltigheim, France, Tel. +33 388 191 510; email: f.pelascini@critt.fr*
[c]*Epteau, 1 rue Grange Peyraud, 01360 Loyettes, France, Tel. +33 472 930 050; email: dhurlaborde@epteau.com*

Received 21 May 2015; Accepted 25 January 2016

ABSTRACT

Combining low-grade solar heat source and polymer materials allows seawater desalination while fossil fuels are saved and use of chemicals against fouling and corrosion is reduced. SOLar Multi-Effect Desalination (SOLMED) project meets recommendations of the US National Research Council, Middle East Desalination Research Center of Oman and Australian Desalination research roadmap regarding the future of desalination. Water cost reduction and development of technologies with low environmental impact are the main guidelines of SOLMED. Low-temperature multi-effect distillation (LT-MED) is well known to be the most efficient distillation process. Coupling LT-MED with a solar heat source downstream of a CSP power plant allows to benefiting of a low marginal cost heat source. This paper presents the advancement of SOLMED project in which a full-polymer material MED desalination prototype is developed to be used with a low-temperature heat source. Operation and coupling parameters are calculated in order to minimize electricity and water total production cost.

Keywords: Desalination; Distillation; Multi-effect; Low temperature; Polymer; Solar energy

1. Introduction

Low-temperature distillation for seawater desalination is a field of investigation to develop the use of low-cost heat sources. As this decreases water price, distillation competitiveness is enhanced. When multi-effect distillation process is used, hybridation with another process such as an absorption heat pump [1] or an adsorption system [2,3] is an additional improvement. Anyway, as distillation is operated at low temperature, the technology developed in SOLar Multi-Effect Desalination (SOLMED), based on polymers, can be used.

A full description of SOLMED project goals and characteristics has been given by authors in a previous paper [4]. The three main features are reminded hereafter:

(1) Low-temperature multi-effect distillation (LT-MED) process on vertical tubes is used to ensure thermal efficiency and flexibility to operating conditions.

*Corresponding author.

Presented at EuroMed 2015: Desalination for Clean Water and Energy Palermo, Italy, 10–14 May 2015. Organized by the European Desalination Society.

(2) Use of thin wall tubes (50 μm) made of polymer as heat transfer surface brings low cost of material and an excellent behaviour in corrosive and fouling conditions.
(3) Solar heat source is used to minimize carbon footprint. To reduce solar heat cost, SOLMED is coupled downstream of a CSP power plant. Marginal cost of energy is very low, as for any dual purpose plant.

SOLar Multi-Effect Desalination (SOLMED) project meets recommendations of the US National Research Council [5,6], Middle East Desalination Research Center of Oman [7] and Australian Desalination research roadmap [8] regarding the future of desalination. The work presented in this paper is related to prototyping, thin-wall tubes characterization, including ageing of polymer stressed by temperature and strength, and techno-economic evaluation of LT-MED coupled with a power plant.

2. Prototyping of SOLMED

SOLMED has been designed according to Fig. 1. It uses the well-known MED process. Heat transfer surface is composed of vertical polymer tubes. SOLMED comprises four evapo-condensers plus a final condenser; the effects number is five. To have only one brine recycling pump, brine and vapour circulation are co-current. Valves are used to adjust pressure difference and water levels in evaporator shells along brine and condensate flows. In the future, orifice plates could replace the valves. As no seawater is available on site, the prototype is operated with tap water during debugging step and then with synthetic seawater prepared according to Kester et al. [9]. Solar heat or low-grade heat source is simulated with an electric heater. This allows simulating of available heat power profiles, and also of a full sunny day on a shortened experiment time. Vapour feeding the first effect is produced in a flash vessel from distillated water taken on fresh water production flow. Operating parameters and expected results are summarized in Table 1, for nominal load and half load.

Photos of Fig. 2 show the prototype connected to different utility skids. Internals of each evaporator are composed of flexible thin tubes and connecting parts to fit them with tubular sheets. In addition to connecting tubes and sheets, these parts ensure a number of functions such as seawater distribution at the top of the tubes, compensation of tubes expansion and air venting of tubes on condensation side.

3. Tubes characterization

3.1. Metrology of tubes

Metrology of polymer tubes is an important control step of prototyping. A first-level control is operated during fabrication by extrusion blowing to adjust

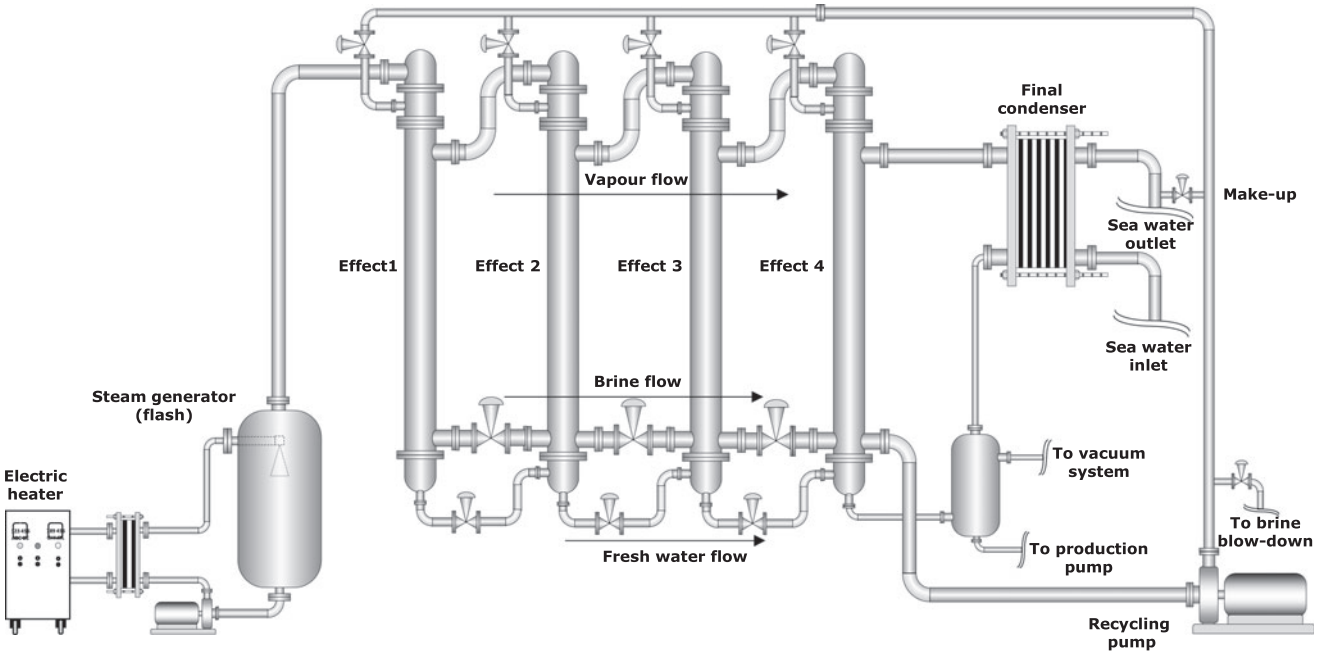

Fig. 1. Simplified flow sheet of SOLMED prototype.

Table 1
SOLMED prototype main characteristics

	Full capacity	Half load
Effects number	4 + 1	4 + 1
Water head temperature	76°C	53°C
Hot water flow rate	6.4 m^3/h	5.4 m^3/h
Seawater temperature	25°C	25°C
Seawater flow rate	8.2 m^3/h	8.2 m^3/h
ΔT head evaporator	12.0°C	6.0°C
ΔT between effects	3.7°C	1.9°C
ΔT final condenser	11.8°C	5.9°C
Evaporator thermal power	60 kW	30 kW
Condenser thermal power	50 kW	25 kW
Targeted GOR	4.0	4.0
Head evaporator surface	1.5 m	1.5 m
Evapocondensers surface	7.4 m	7.4 m
Final condenser surface	1.3 m	1.3 m
Number of tubes/effect (L = 3.7 m ϕ32 mm)	19	19
Fresh water production	380 L/h (9.1 m^3/d)	188 L/h (4.5 m^3/d)
Make-up flow rate	760 L/h	376 L/h
Brine flow rate (@conc. factor 2)	380 L/h	190 L/h
Air vent flow rate	8 m^3/h	11 m^3/h
Air vent pressure	50 mm Hg	36 mm Hg

process parameters. Final control is done to accept or reject a part or the totality of a fabrication lot. Critical parameters and related results are:

(1) Thickness: an 8-point method (Fig. 3(a)) on tube perimeter is used (4 positions along 3 samples: 96 points over 1,000 m, measured with a micrometer). Results are given in Fig. 4 and Table 2. Mean thickness (56 μm) is clearly out of specification (50 μm) with a shift towards high values. The consequence is a higher wall thermal resistance. Thickness difference of the two half peripheries (points 1–4 and 5–8, visible on Fig. 4) results of eccentricity of the punch in the extrusion die. A new die design is planned to correct this point and process parameters adjustments such as pull rate will reduce the thickness.
(2) Diameter: as the tubes must fit with the tubes sheets using machined parts, the smallest tube (smallest diameter) must be compatible with the biggest part (largest diameter). Tubes being thin and flexible, diameter cannot be directly measured. Tubes are flattened and their width is measured with a calliper. Outer and inner diameters are then calculated with relations (1) and (2):

$$D_{out} = 2\,W_F/\pi \quad (1)$$

$$D_{in} = D_{out} - 2\,e \quad (2)$$

Width is measured for five positions (Fig. 3(b)) on five tube samples (2.4 m, 25 points over 12 m). Fig. 5 and Table 2 show results. Tube diameters match with specification.

(3) Bending: measurement method is shown on Fig. 3(c) and results in Table 2. As measurements are related to a 2 m tube length, extrapolation to a 3.7 m tube is geometrically calculated assuming that the tube shape is a circle arc. Finally, bending is calculated within 35 and 50 mm for a length of 3.7 m. As tubes pitch is only 45 mm, two adjacent tubes of an evaporator can stick one to the other. A grid system keeping the space between the tubes is included inside each evaporator's shell.

3.2. Thermal properties of tubes

Thermal properties are related to thermal conductivity, thermal expansion and shrinkage. Thermal conductivity has been measured by hot disc method although this method is not recommended for thin insulating layers. Nevertheless, measurements with different sample thicknesses allow corrections, the main one being thermal contact resistance between probe and sample. Table 3 shows that measurement results meet expected values. Material A and B are both copolymers based on polyolefin resins. It has to be noticed that expected values from literature or

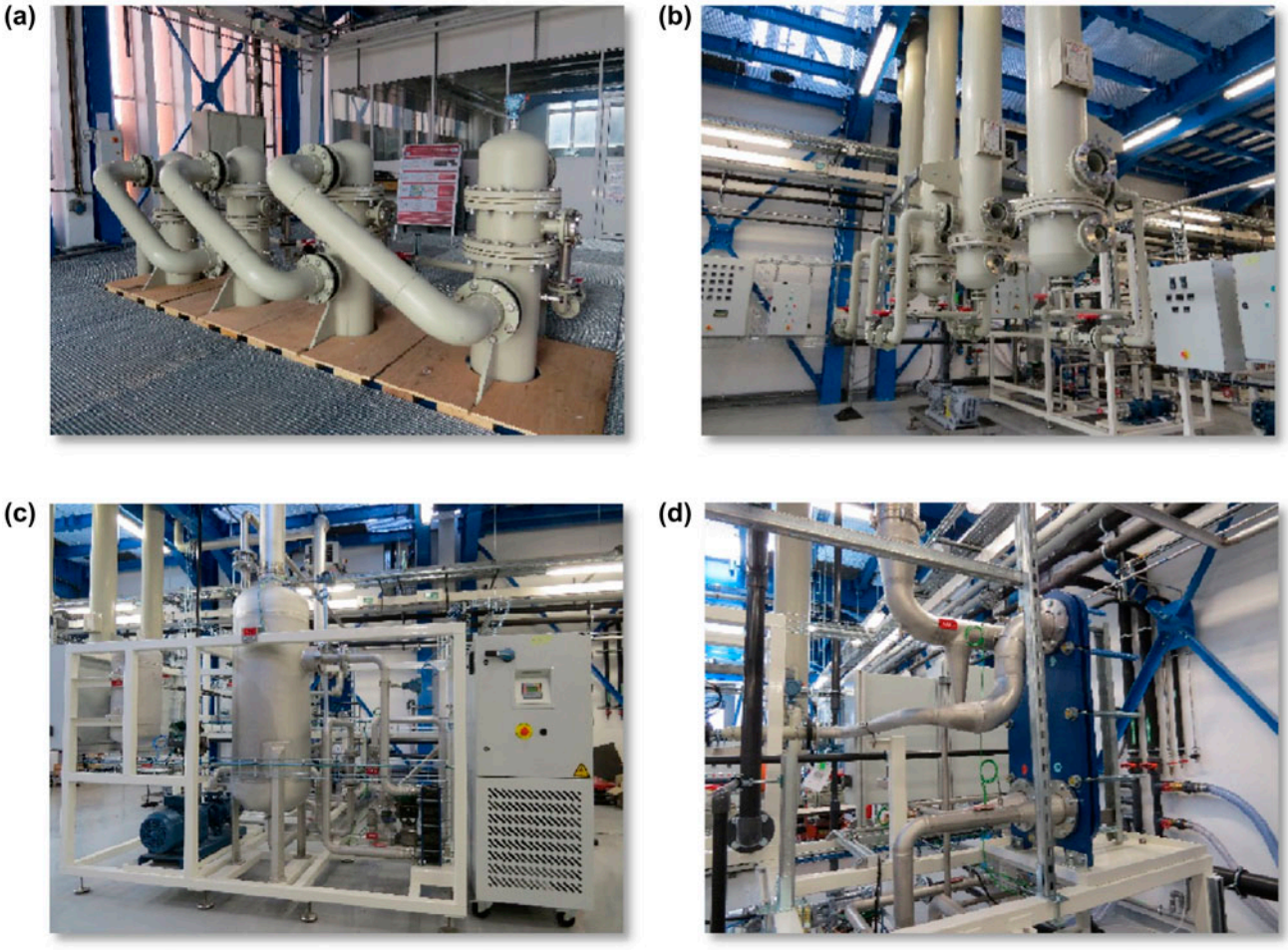

Fig. 2. (a) Upper view, (b) bottom view, (c) heater and steam generator skid and (d) final condenser skid.

suppliers data sheets are related to thick samples; it is well known that thin extrusion decreases transverse thermal conductivity.

Another critical thermal property of tubes is the linear thermal expansion coefficient of material. Polymers are very sensitive to temperature regarding variations of dimensions. Polymers expansion is generally 10 times more than metals one in the same conditions. In the case of long tubes, it is mandatory to use a mechanical system able to compensate expansion. Sizing of this system requires prediction of tube length variations during operation when the temperature varies. Expansion has been measured on wetting and ageing test equipment presented in the next section of this paper. Initial cold tubes length is 2.4 m, length in operation conditions has been measured at 65 and 80°C. Thermal expansion coefficient is then calculated with relation (3) (Table 4).

$$a = \frac{\Delta l}{l_0 \, \Delta T} \tag{3}$$

Shrinking is the ability of polymer to become irreversibly shorter when it is heated. Expansion is reversible, not shrinking, but it is limited; it occurs only during the first temperature ramp. Consequently, material must be stabilized before assembling or shrinking must be taken into account when cutting the tubes. Table 5 indicates measured shrink for material A and material B and Fig. 6 shrinking kinetic of material B. Measurements are related to a sample with an initial length of one metre heated in an oven. Length is measured at room temperature after cooling the sample. This shows that material stabilization is reached after about 13 h.

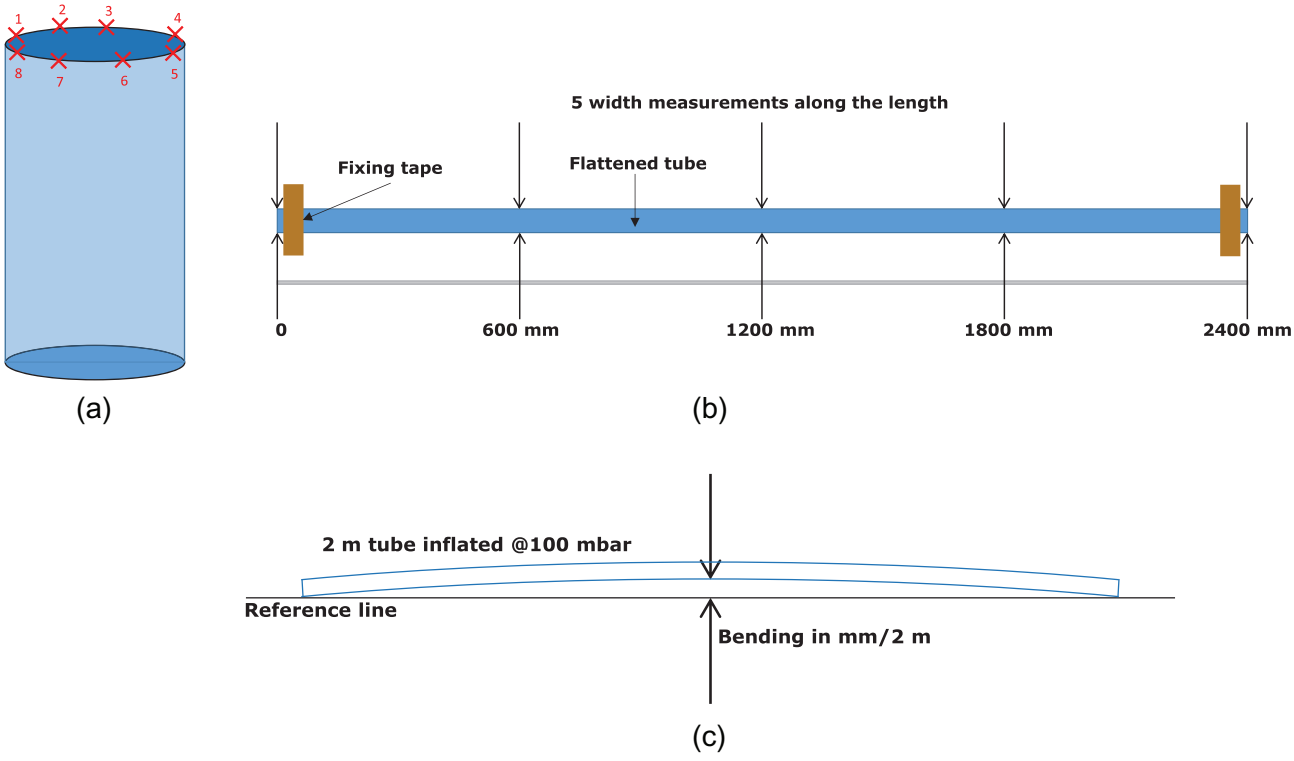

Fig. 3. Protocol of metrology: (a) wall thickness, (b) width of flattened tube and (c) bending.

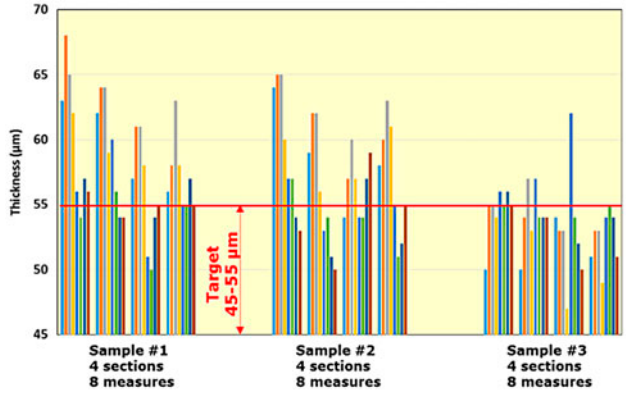

Fig. 4. Thickness measurements.

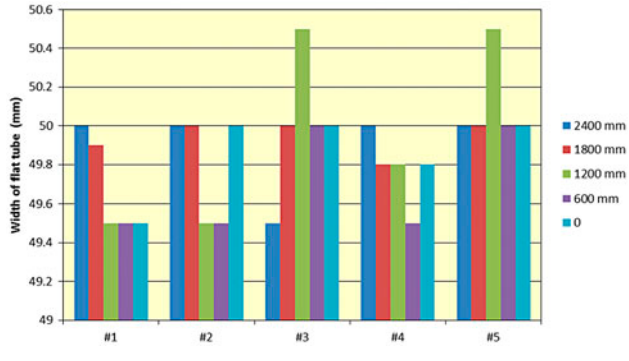

Fig. 5. Flattened tubes width.

Table 2
Metrology results (σ: standard deviation)

	Width (mm)	Outer diameter (mm)	Thickness (µm)	Bending @100 mbar, 20°C
Target	50 ± 0.5	31.8 ± 0.3	50 ± 5	<10 mm/4 m
Mean value	49.9 σ 0.3	31.8 σ 0.2	56 σ 4	12 mm (4 tubes) → 48 mm/4 m
Minimum	49.5	31.5	47	10 mm/2 m → 40 mm/4 m
Maximum	50.5	32.1	68	14 mm/2 m → 56 mm/4 m

Table 3
Thermal conductivity measurements

	Sample thickness (μm)	λ 20°C (W/m K^{-1})	Expected value (W/m K^{-1})
Round #1 Mat A	57, 62, 85, 91	0.26 σ 0.02	0.26 (0.3–0.4 in the range 40–93°C)[a]
Round #2 Mat A	53, 64, 76	0.30 σ 0.03	
Round #3 Mat B	50	0.13	0.15–0.21 (25°C)[b]

[a]Supplier data [10].
[b]Literature data [11].

Table 4
Coefficient of linear thermal expansion

	LTE coefficient (m/m K^{-1})	Expected value (m/m K^{-1})
Mat B @80°C	2.1×10^{-4}	$0.7–1.7 \times 10^{-4}$[a]
Mat B @65°C	1.8×10^{-4} σ 0.2×10^{-4}	

[a]Literature data [11].

Table 5
Shrinkage (σ: standard deviation)

	Shrinkage %	Expected value %
Mat A @85°C 10 h	0.4 σ 0.1	–
Mat B @75°C 14 h	0.7 σ 0.03	1–2[a]

[a]Literature data [12].

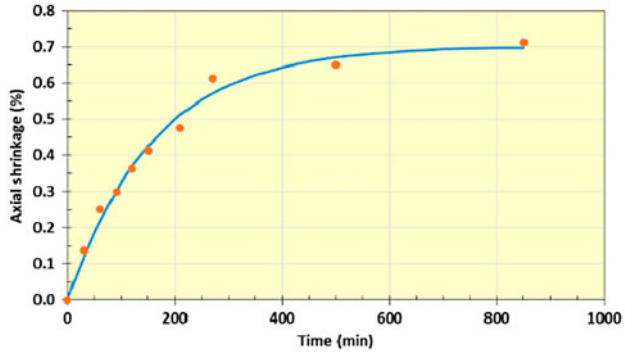

Fig. 6. Tube axial shrinking at 75°C.

Fig. 7. Ageing and wetting test rig of polymer tubes.

3.3. *Tubes wetting*

Tube wetting is a key parameter to ensure operation of the evaporator. A test rig dedicated to wetting and ageing of tubes has been built (Fig. 7) and described in a previous paper [4].

It has been observed that new tubes are rather hydrophobic, but as measured by A. Gonda [13], contact angle on evaporation side decreases with time from about 100° to 80°. Gonda has shown that this last value allows a full wetting of the tubes. Fig. 8 shows the evolution from a dry new tube (8a) to a fully wetted tube (8d). Time between the two figures is one

day. An intermediate state shown in 8c is the film formation from the tube top, under the distribution system, with a slow progression towards the bottom. Evolution of wettability is probably the result of a very slight fouling (not visible) of the tubes surface changing the surface properties. This has no effect on future heat transfer but modifications of surface properties are decisive. It must be mentioned that this test has been carried out at nominal operation temperature (65°C) without inside steam condensation, the circular shape of tubes is ensured by an internal air pressure. Demineralized water is demineralized flows outside the tubes in stainless steel closed circuit. Using an open seawater circuit reduces the wetting time [13].

3.4. Tubes ageing

Ageing of thin wall tubes is also a critical parameter; as wall thickness is about 50 μm, strengths may be high even if pressure difference is rather low. Figs. 9(a) and (b) shows what happens when ageing is strongly accelerated by temperature and stress. A tube made of material B has been heated at 80°C, while radial strength was maintained at 3.2 MPa with an internal air pressure. Rapidly, a "bubble" appears, probably in a thinner region. After only 100 h, the tube bursts. This is the result that the radial strength is higher than the axial one (3.2 vs. 1.9 MPa) and the radial resistance is slightly lower than the axial one (21 vs. 26 MPa @20°C, result of traction tests on a 60 μm thickness sample). At the outlet of the extrusion equipment, the tubes are flattened and rolled creating two folds on the sides. Breaking occurs in the plain wall, not in a folded region.

Ageing is the result of many parameters. Oxygen, short wavelength light and combination of both are accelerating factors. Fortunately, desalination systems work with deaerated water under reduced pressure, without any light source; polyolefins are not sensitive to seawater corrosion as they are chemically stable. Nevertheless, material is stressed; temperature and strength limit their lifetime. Mechanism of failure is a combination of creeping and fatigue behaviour. Investigation about lifetime prediction is engaged. It is easy to get mechanical properties at ambient temperature and determine initial strength yield; but lifetime diagrams are rather rare, especially with temperature effects, in suppliers' data sheets. Available data about polymer B lifetime taking into account strength and temperature come from two references [14] and [15].

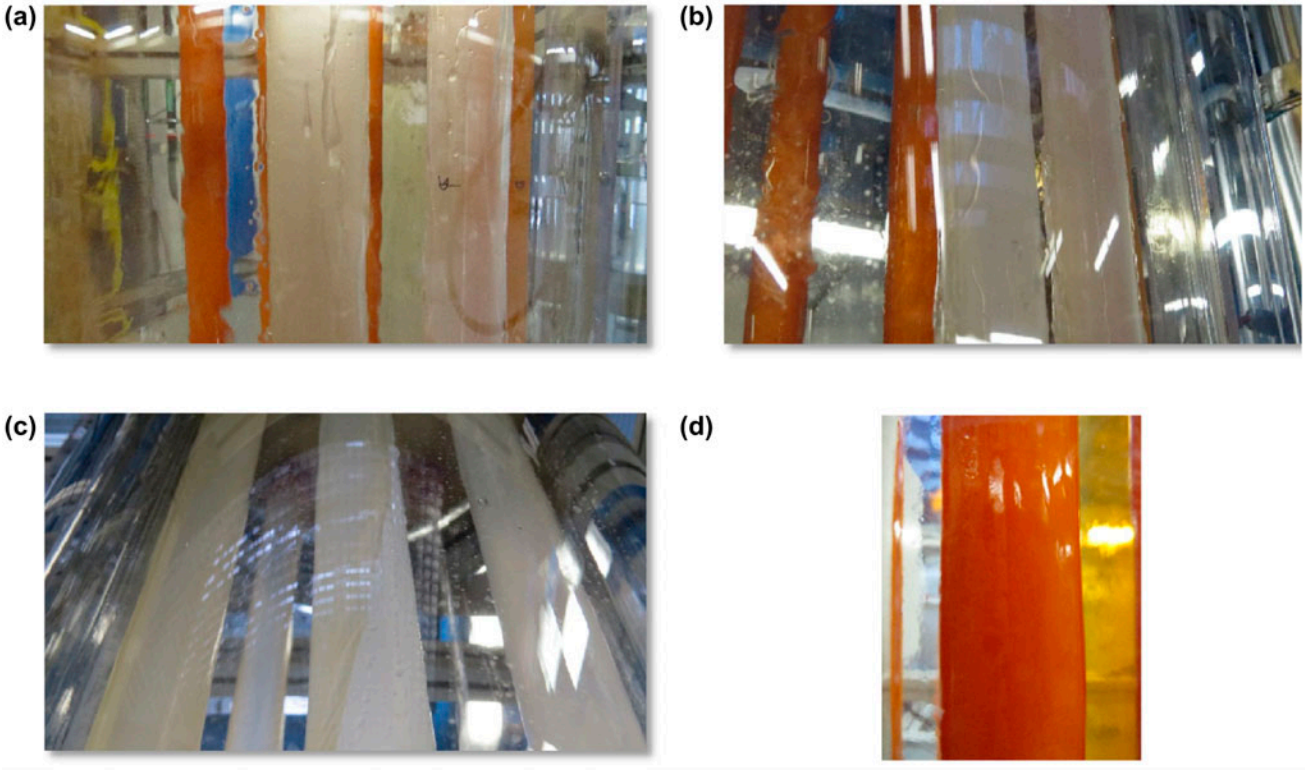

Fig. 8. (a) Absence of wetting, drops and rivulets, (b) multiplication of moving rivulets, (c) wetting progresses and (d) full wetting (dye to visualize water film).

Fig. 9. (a) Apparition of bubble and (b) definitive break of tube.

They have been established for only two temperatures, at 20 and 100°C and for thick samples, not for films. To determine lifetime in other conditions, Avrami model has been used [16,17]. Fig. 10 is the plot of linearization parameters for Avrami Eq. (4).

$$\ln\left[-\ln\left(1-\frac{\sigma_0-\sigma_t}{\sigma_0}\right)\right]=\ln K+n\ln t \tag{4}$$

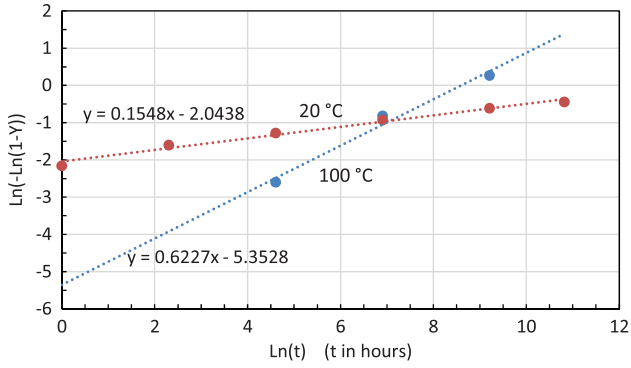

Fig. 10. Avrami plot for data of polymer B.

Linearity shows that ageing follows Avrami equation and allows determining K and n values (intercept and slope).

Assuming that kinetic constant K follows the Arrhenius law, strength at yield and lifetime are given by Eqs. (5) and (6):

$$\sigma_t=\sigma_0\exp\left[-K_0\,t^n\exp\left(-\frac{E_A}{RT}\right)\right] \tag{5}$$

$$t=\sqrt[n]{\frac{\ln\left(\frac{\sigma_t}{\sigma_0}\right)}{-K_0.\exp\left(-\frac{E_A}{RT}\right)}} \tag{6}$$

Temperature dependence of ageing is taken into account in kinetic constant, but Figs. 9 and 10 show clearly that σ_0 and n are also temperature dependent. Again, Arrhenius law is used to describe this dependence. Finally, a predictive model based on interpolation gives lifetime for given temperature and strength. Fig. 11 shows predicted lifetime at 65°C (grey dot line), strength range of ongoing tests (black lines) and current points when this paper is published (black square marks). Accelerated test at 80°C (brown dot), traction and blowing test at 20°C (grey dots) are also represented. Fig. 11 shows that theoretical lifetime at 65°C exceeds 11 years. The objective is to check if another uncontrolled parameter does not make it shorter in normal operating conditions. As shown by accelerated tests at 80°C, actual time to failure is only 100 h when model predicts about 3 years. Uncontrolled parameters may be local or repetitive defects on the tubes, brittleness along tube side on fold lines when the tube is rolled after extrusion, local wall thinning due to misalignment of the punch in the extrusion die, or any other unidentified reason.

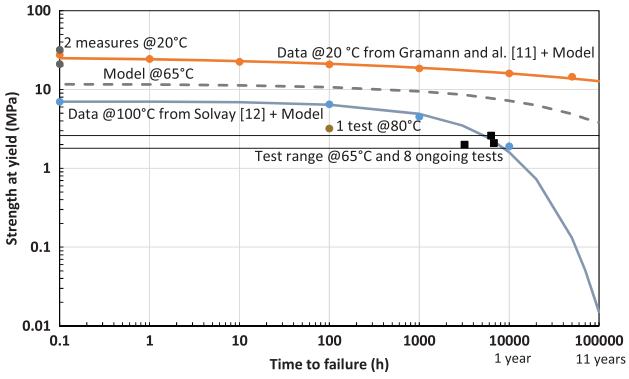

Fig. 11. Ageing model and prediction for 65°C.

4. Evaluation of coupling scheme with solar heat source

The study of coupling a desalination plant to a solar heat source consists in production of electricity and water at minimum total cost. Water production can be chosen to be coherent or not with electricity production. Reference case is a 10 MW electric net Rankine power plant. Desalination plant is calculated and optimized to deliver water and electricity at minimum total cost. Fig. 12 details the simplified Rankine model with two expansion stages and coupling with desalination unit. Desalination head evaporator is one Rankine cycle condenser. Main hypothesis are listed in Table 6. Different scenarios are possible:

(1) No desalination (reference scenario SC0).
(2) Desalination plant is the power plant condenser, all available thermal power is used for desalination; condensation temperature and effects number are minimum (SC1).
(3) A fraction of thermal power taken during expansion is used to produce water in coherence with electric power; condensation temperature and taken vapour fraction are optimized (SC2).

Taking vapour during expansion makes that thermal energy cost is linked to the oversizing of solar heat source and power block to ensure an identical electricity production. By the way, electricity cost increases.

Without desalination, production of 10 MW electric requires 50.3 MW of heat, while expander delivers 11.1 MW of gross mechanical power and condenser receives 39.2 MW.

When all available thermal power is used for desalination at 40°C (outlet condenser temperature plus pinch), only two effects requiring available 39.2 MW can be used. About 2,750 m^3/d of water are produced at 1.42 €/m^3 and total daily cost is 39,900 € (electricity @0.15 €/kWh). Water production cost can drop down to 0.89 €/m^3 with a total daily cost of 14 450 € (electricity @0.05 €/kWh). Electricity production cost represents, respectively, 90 and 80% of total cost.

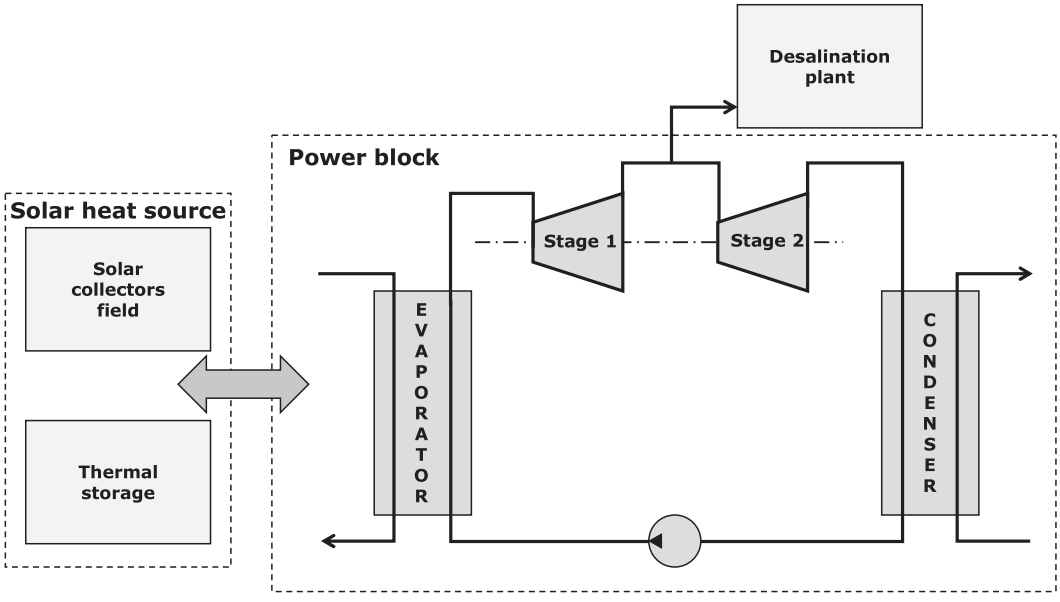

Fig. 12. Simplified model of dual purpose solar plant.

Table 6
Input data for electricity and water production

Rankine cycle	
Electric net power	10 MW
Heat source outlet temperature	260°C
Evaporator and condenser pinch	5°C
Seawater outlet temperature	35°C
Carnot shift	10%
Expander efficiency	60%
Converter efficiency	95%
Rankine pump fraction power	5%
Desalination	
Reference electricity cost	0.15 €/kWh 0.05 €/kWh
Minimum ΔT between effect	2.5°C
Head temperature	Variable
Heat cost	Calculated
Operation	24 h/d
Desalination operating cost	As usual
Desalination capital cost (discount rate 0)	As usual
Plant lifetime	25 y

To fit water production with power (1 kW/(m^3/d) = 1,000 m^3/(d MW) [18]), desalination capacity must be 10,000 m^3/d. Scenario SC1 does not meet this requirement as only 2 750 m^3/d of water can be delivered.

Scenario SC2 is the sole able to produce 10,000 m^3/d. Fig. 13 analyses this scenario. Total daily cost is given in function of taken vapour temperature. Calculations are made for two reference electricity costs at production: expensive option (a) such as solar electricity from CSP and cheap option (b) at industrial tariff. Vapour fraction increases when temperature decreases but this last one cannot drop below 57°C, otherwise all available thermal power is consumed without reaching targeted production. For each vapour temperature, the effects number leading to a minimum total cost has been searched; it may mismatch with minimum water cost as water is only a small fraction of total cost (20–30%). Desalination effect on electricity cost is important as it rises of about 11% to produce water. Then, total daily cost is not very sensitive to temperature increase: +2 to +3%, because fraction to take decreases when temperature increases; without any surprise, the minimum cost is clearly when vapour is taken at the lowest temperature.

5. Conclusion

SOLMED is a new desalination technology applied to a well-known robust process (LT-MED). Its main characteristic is to use thin wall flexible polymer tubes as heat transfer surface. Tubes with a wall thickness of 50 μm have been manufactured with a polyolefin-based material. If their characteristics allow to use them to start up the prototype, continuous improvement of their properties is engaged to match with all specifications related to dimensions, mechanical and thermal properties. In parallel, wetting and ageing tests are ongoing. It has been proved that if polymers are hydrophobic at start-up, they become wettable on evaporation side within one day. Accelerated ageing tests have shown the weak point of mechanical resistance, leading to the burst of tested tube and premature failing. Long-time ageing tests are ongoing; no break appears after 9 months representing only 2% of theoretical massive material lifetime. But practical lifetime is probably shorter. A coupling scheme of SOLMED with a CSP power plant using usual economic data of MED, shows that the total supplying

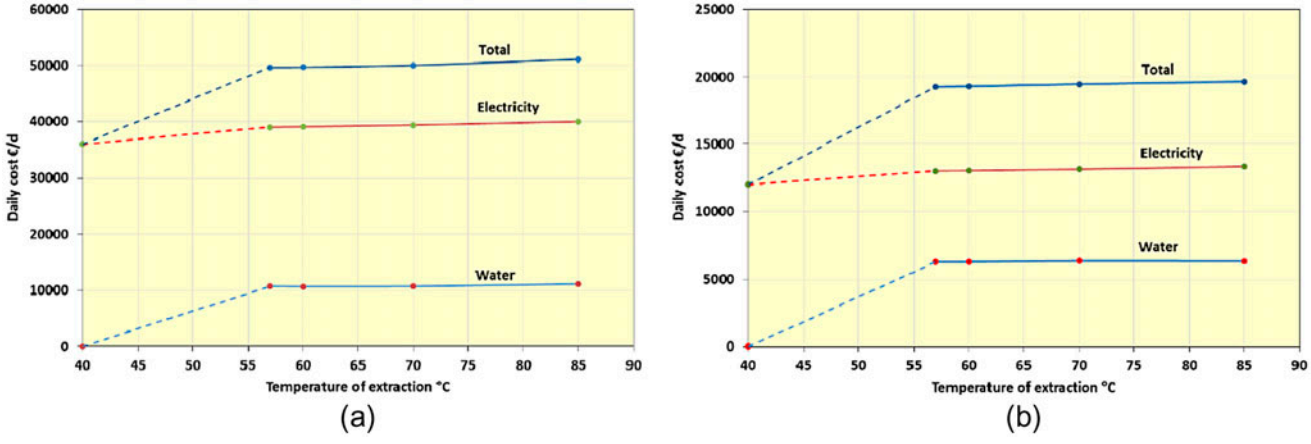

Fig. 13. Total daily cost—reference electricity cost 0.15 €/kWh (a), 0.05 €/kWh (b) −10 MW + 10,000 m^3/d.

cost of electricity and water is only slightly affected by temperature of the taken vapour on a Rankine cycle. The reason is that power generation is the main contribution to the total cost and increasing the temperature decreases in the same time the fraction of vapour to be taken.

SOLMED is funded by the French National Research Agency under project reference ANR-11-SEED-002. It benefits of support of the energy clusters Tenerrdis and Capenergies. Developments are carried out by a consortium composed of CEA-Liten (coordinator), Epteau company, CRITT-Matériaux Alsace, CNRS-LRGP laboratory and Grenoble Ecole de Management. After the ongoing phase related to prototyping and proof of concept, a demonstration step is planned in the frame of a partnership.

Notations

a	—	thermal expansion coefficient (m/m K^{-1})
D_{in}	—	tube inner diameter (m)
D_{out}		tube outer diameter (m)
W_F	—	tube width in flat position (m)
E_A	—	energy of activation (J/mol)
e	—	tube wall thickness (m)
K	—	ageing kinetic constant (t^{-n})
K_0	—	constant in Arrhenius kinetic law (t^{-n})
l_0	—	reference length for expansion (m)
n	—	Avrami exponent, dimensionless
R	—	gas constant (J/mol K^{-1})
t	—	ageing time (h)
Δl	—	length increase during thermal expansion (m)
ΔT	—	temperature increase for expansion (K)
σ_0	—	initial material strength at yield (MPa)
σ_t	—	current material strength at yield (MPa)

References

[1] B. Milowr, E. Zarza, Advanced MED solar desalination plants. Configurations, costs, future—Seven years of experience at the Plataforma Solar de Almeria (Spain), Desalination 108 (1996) 51–58.
[2] M.W. Shahzad, K.C. Ng, K. Thu, Future sustainable desalination using waste heat: Kudos to thermodynamic synergy, Environ. Sci. Water Res. Technol. 2 (2016) 206–212, doi: 10.1039/c5ew00217f.
[3] M.W. Shahzad, K. Thu, Y.-d. Kim, An experimental investigation on MEDAD hybrid desalination cycle, Appl. Energy 148 (2015) 273–281.
[4] P. Bandelier, J.J. d'Hurlaborde, F. Pelascini, M. Martins, A. Gonda, D. Alonso, M. Berlandis, F. Pigni, SOLMED: Solar energy and polymers for seawater desalination, Desalin. Water Treat. 55(12) (2015), doi: 10.1080/19443994.2014.939500.
[5] Review of the Desalination and Water Purification Technology Roadmap, Water Science and Technology Board, National Research Council of the National Academies, National Academies Press, Washington, DC, (2004).
[6] A.K. Zander, Desalination: A National Perspective, National Research Council, Committee on Advancing Desalination Technology, National Academies Press, Washington, DC, 2008.
[7] Middle East Desalination Research Center MEDRC, Sultanate of Oman, Research Program (2014). Available from: <http://www.medrc.org/>.
[8] T.E. Hinkebein, Australian Desalination Research Roadmap, Murdoch University, National Centre of Excellence in Desalination, 2012.
[9] D.R. Kester, I.W. Duedall, D.N. Connors, Preparation of artificial seawater, Limnol. Oceanogr. 12(1) (1967) 176–178.
[10] Chevron Phillips Chemical Company LP, September, (2002).
[11] M. Biron, Thermoplastics and Thermoplastic Composites, Elsevier Ltd., Amsterdam, 2007, pp. 258–259.
[12] Ineos Olefins & Polymers USA, Typical Engineering Properties, 2014.
[13] A. Gonda, D. Alonso, V. Renaudin, P. Bandelier, SOLMED: Heat transfer characterization, EuroMed 2015, Desalin. Clean Water Energy, Palermo, Italy, May 10–14 (2015).
[14] P.J. Gramann, J. Cruz, J.A. Jansen, Lifetime Prediction of Plastic Parts—Case Studies, ANTEC Proceedings, Orlando, 2–4 April, vol. 2, 2012, pp. 1313–1318.
[15] Commercial documentation, Solvay.
[16] A.S. Maxwell, W.R. Broughton, G. Dean, G.D. Sims, Review of accelerated ageing methods and lifetime prediction techniques for polymeric materials, National Phys. Lab. Rep., DEPC MPR 16 (2005) 24–25.
[17] A.G. Marangoni, On the use and misuse of the Avrami equation in characterization of the kinetics of fat crystallization, J. Am. Oil Chem. Soc. 75(10) (1998) 1465–1467.
[18] O.A. Hamed, G.M. Mustafa, K. Bamardouf, H. Al-Washmi, SWCC MSF desalination plants—Current status and future prospects, 6th Saudi Engineering Conference, KFUPM, Dhahran, Saudi Arabia, 14–17 December 2002.